Newman-Norlund, R., Gibson, M., Johnson, L., Teghipco, A., Rorden, C., Bonilha, L., & Fridriksson, J. (2023). Cerebellar Atrophy and Language Processing in Chronic Left-Hemisphere Stroke. Neurobiology of Language, Advance publication. https://doi.org/10.1162/nol_a_00120.

Cerebellar Atrophy and Language Processing in Chronic Left-Hemisphere Stroke

Roger D. Newman-Norlund[1], Makayla Gibson[1], Lisa Johnson[2], Alex Teghipco[1], Chris Rorden[1], Leo Bonilha[3], Julius Fridriksson[2]

[1] University of South Carolina, Department of Psychology, College of Arts and Sciences, Columbia, SC
[2] University of South Carolina, Department of Communication Sciences, Arnold School of Public Health, Columbia, SC
[3] University of South Carolina, School of Medicine, Columbia, SC

Key Words: cerebellum, chronic, stroke, brain, language

Date of Initial Submission: January, 2022

Running Title: CEREBELLUM AND CHRONIC STROKE

Number of words, 1964
Number of Figures: 3
Number of Tables: 1 (+ 6 many supplementary tables)

Declarations

Corresponding author: Roger D. Newman-Norlund, rnorlund@mailbox.sc.edu

Conflict of Interest: The authors do not report any conflicts of interest.

Funding Source: NIH C-STAR P-50 grant (PI, Fridriksson), NIH ARCquery supplement (PI Rorden) ,University of South Carolina (USC) Excellence Initiative (PI, Fridriksson)

Availability of data and materials: The datasets generated and/or analyzed during the current study are available from the corresponding author upon request.

Code availability: All code used is publicly available or available upon request.

Ethics approval: This study was approved by the University of South Carolina's Institutional Review Board

Consent to participate: Written informed consent was obtained from all individual participants included in the study.

Consent for publication: I, Roger David Newman-Norlund, give my consent and the consent of my coauthors, for the publication of the submitted article.

Abstract

Chronic stroke results in significant downstream changes at connected cortical sites. However, less is known about the impact of cortical stroke on cerebellar structure. Here, we examined the relationship between chronic stroke, cerebellar volume, cerebellar symmetry, language impairment, and treatment trajectories in a large cohort (N = 249) of chronic left hemisphere (LH) stroke patients with aphasia, using a healthy aging cohort (N = 244) as control data. Cerebellar gray matter volume was significantly reduced in chronic LH stroke relative to healthy control brains. Within the chronic LH stroke group, we observed a robust relationship between cerebellar volume, lesion size, and days post-stroke. Notably, the extent of cerebellar atrophy in chronic LH patients, particularly in the contralesional (right) cerebellar gray matter, explained significant variability in post-stroke aphasia severity, as measured by the Western Aphasia Battery–Revised (WAB-R), above and beyond traditional considerations such as cortical lesion size, days post stroke, and demographic measures (age, race, sex). In a subset of participants that took part in language treatment studies, greater cerebellar gray matter volume was associated with greater treatment gains. These data support the importance of considering both cerebellar volume and symmetry in models of post-stroke aphasia severity and recovery.

Introduction

A stroke occurs every 40 seconds in the United States and the total economic burden of stroke is estimated to reach over 240 billion USD per year by the year 2030. (Heart and Stroke Association Statistics; Ovbiagele et al. 2013) Aphasia, which most commonly results from insult to the left middle cerebral artery (MCA), can have a profound effect on the quality of life (Spaccavento et al. 2014) and mental health (Gainotti 1997) of those affected as well as their caregivers (Michallet et al. 2003). While lesion size and location are typically reliable predictors of aphasia severity and behavioral outcomes (Thye and Mirman 2018; Busby et al. 2023; Kristinsson et al. 2022), researchers have also identified important functional and structural changes at cortical sites connected to, but distal from, the original lesion site (Baldassarre et al., 2016; Kalinosky et al., 2017; Tang et al., 2016; Wilmskoetter et al., 2019, 2021). However, the relationship between structural integrity of the cerebellum, aphasia severity and the potential for recovery of language abilities in chronic left hemisphere (LH) stroke has not been systematically evaluated.

The lack of data relating cerebellar integrity to stroke is striking given what is known about the interconnectedness of the cerebellum and putative language areas (Justus, 2004; Leiner et al., 1993; Silveri et al., 1994; Zettin et al., 1997). Based on these and other studies, cerebellar lesions are hypothesized to impact human language via poly-

synaptic pathways related to, but not overlapping with, core linguistic systems (Fiez, 2016; Moberget & Ivry, 2016). Complementary evidence for cerebellar involvement in language processing comes from various functional imaging studies. For example, Petersen and colleagues, used positron emission tomography (PET) to identify right cerebellar activation during verb generation, which, at the time, was thought to reflect retrieval and preparation of linguistic motor responses. Data from functional magnetic resonance imaging (fMRI) studies provides further evidencethat the cerebellum is critically involved in language, (Desmond and Fiez 1998; Xiang et al. 2003; Booth et al. 2007) with a recent meta-analysis concluding that specific regions of the cerebellum, including Crus I, Crus II as well as Lobules VI and VIIA, are particularly integral to language function (Mariën and Manto 2015).

In the current study, we leveraged a large and relatively homogeneous population of chronic LH stroke survivors with aphasia (N = 249), along with control data from our local Aging Brain Cohort (Newman-Norlund, R.D. 2021) (N = 244), to examine the relationship between cerebellar changes in individuals with aphasia as a result of chronic LH stroke (**Table 1**, Demographics). Cerebellar structural integrity was quantified as 1) gray matter volume, 2) white matter volume and 3) volumetric symmetry. Based on prior research, we hypothesized that chronic LH stroke would be accompanied by significant reductions in cerebellar gray and white matter volume, particularly in the contralesional hemisphere of the cerebellum, with the extent of these

cerebellar changes being associated with severity of reported clinical impairments (i.e. aphasia severity) as well as clinical prognosis (i.e. recovery of language abilities following treatment).

Methods

Participants

Participants included in the following analyses were enrolled over various studies from the Center for the Study of Aphasia Recovery (C-STAR). Chronic left hemisphere stroke participants were recruited between the ages of 21 and 80, and were considered eligible for study after 12 months post-onset of an ischemic or hemorrhagic stroke. Individuals excluded from participation include those presenting with contraindications of MRI, bilateral or RH stroke, or pre-existing major neurological disorders (such as Parkinson's or Multiple Sclerosis). Information regarding the healthy cohort used for these analyses can be found in the Aging Brain Cohort Repository (Newman-Norlund, R.D. 2021).

Imaging Data Collection

Neuroimaging data were acquired as part of participation in one of multiple NIH funded and/or internally funded grants conducted over a period of 16 years. Participants were included in the present study if their participation involved collection of a high-resolution T1-weighted structural MRI scan. For clinical populations, MRI data were acquired

using a Siemens 3T scanner which was upgraded from a Prisma Trio to a Prisma FIT in 2016. Properties of the whole-brain 3D GR\IR sequence used in the clinical sample were as follows: repetition time (TR) = 1160 ms, inversion time (TI) = 600 ms, echo time (TE) = 4.24 ms, flip angle = 15°, 256 × 256 x 192 isotropic voxels. MRI data in healthy participants was acquired using the MGH multi-echo whole-brain MPRAGE T1 sequence with the following parameters: repetition time (TR) 2530 ms, inversion time (TI) = 1100 ms, echo time (TE) = (1.44, 2.9, 4.3, 5.82, 7.28), flip angle = 7°, 256 × 256 x 192 isotropic voxels.

Image Data Processing

Cerebellar volume and total intracranial volume (TIV) were calculated using high-resolution T1-weighted MPRAGE structural MRI images acquired at the McCausland Center for Brain Imaging at the University of South Carolina. All images were processed using MATLAB (Mathworks, 2022b), SPM12 version 7781 (Penny et al., 2011) and the Cat12 (v12.6, 1700) VBM toolbox with default settings (Gaser et al., n.d.). For individuals with stroke, T1-weighted structural images were enantiomorphically healed prior to processing to ensure accurate normalization (Nachev et al., 2008; Yourganov et al., 2018) (see **Supplementary Methods - *Imaging***). For the purpose of this paper, cerebellar structural integrity was operationalized as three separate measures: cerebellar gray matter volume, cerebellar white matter volume, and cerebellar volumetric (both gray and white matter based) lateral symmetry (i.e. left vs right).

Cerebellar volume metrics were derived from each participant using the Cat12 default processing pipeline and normalized by participant's total intracranial volume (TIV). This normalization procedure effectively transformed the data from cubic centimeters to percent total brain volume, a unitless measure that accounts for differences in total intracranial volume among participants (Whitwell et al., 2001). Percent total brain volume, and symmetry measures (see equation below) were used in subsequent statistical analyses reported in this paper. Gray and white matter percent volumes were computed for the left and right cerebellar hemispheres independently, as well as for each of the 34 (17 LH and 17 RH) spatially distinct regions comprising the SUIT cerebellar atlas (Diedrichsen et al., 2009). For the purpose of this paper, we refer to these derived measures, which represent percent total brain volume (see above), simply as GMV and WMV. Cerebellar asymmetry indices for both gray matter volume (GMV LI) and white matter volume (WMV LI) were calculated based on the percent gray and white matter volume described above, using the following standard laterality index equation (Seghier, 2008):

$$\text{GMV } LI = (\%\, Right\ CV - \%\, Left\ CV) \,/\, (\%\, Right\ CV + \%\, Left\ CV)$$

$$\text{WMV } LI = (\%\, Right\ CV - \%\, Left\ CV) \,/\, (\%\, Right\ CV + \%\, Left\ CV)$$

Behavioral Data

Behavioral data included performance on the Western Aphasia Battery-Revised (WAB-R) and the Treated40 object naming task (acquired at two different timepoints - at the time of enrollment, then 6 months following participants' last study intervention session) were acquired as part of C-STAR which is comprised of data from research studies conducted between 2006 and 2022. The Treated40 variable represents treatment-related gains recorded from participants in various C-STAR intervention studies (N = 77). The Treated40 variable was computed by comparing performance on a 40-item picture naming task before and 6 months after a 5-week aphasia treatment which involved both semantic and phonological intervention, with higher numbers indicating greater pre-post improvement, as follows:

[# pictures correctly identified after treatment] - [# of pictures identified before treatment]

Additional details regarding the Treated40 task, its administration, and properties can be found here (Fridriksson et al., 2009) (also see Supplementary Methods - Language Measures).

Results

Based on our hypothesis that cerebellar volume would differ between the healthy and chronic LH stroke groups, we first conducted an uncorrected two-tailed independent

samples t-test for mean differences in total cerebellar volume (GMV+WMV) between the chronic LH group (M = 6.67% TIV, SD = 0.70% TIV) and the healthy control group (M = 7.35% TIV, SD. = 0.70% TIV). The difference between total cerebellar volume in these groups was significant, $t(490) = 10.90$, $p < 0.001$. We subsequently tested for more specific differences in mean GMV and WMV in left and right hemispheres using the same approach (i.e., uncorrected independent samples t-tests). Cerebellar GMV in the left hemisphere was different between the chronic LH stroke (M = 2.56% TIV, SD = 0.30% TIV) and healthy control group (M = 2.81 % TIV, SD = 0.27 % TIV), $t(490) = 9.73$, $p < 0.001$. Similarly, cerebellar GMV in the right hemisphere was different between the chronic LH stroke (M = 2.43% TIV, SD = 0.32% TIV) and healthy control group (M = 2.83% TIV, SD = 0.29% TIV), $t(490) = 14.54$, $p < 0.001$. Although cerebellar WMV in the left hemisphere did not significantly differ between the chronic LH stroke (M = 0.71% TIV, SD = 0.10% TIV), and control group (M = 0.73 % TIV, SD = 0.11% TIV), $t(490) = -1.28$, $p = 0.20$, cerebellar WMV did differ between the chronic LH stroke groups (M = 0.66 % TIV, SD = 0.10% TIV) and healthy control group (M = 0.68 % TIV, SD = 0.11% TIV), in the right hemisphere, $t(490) = 2.21$, $p = 0.028$. As a final, even more fine-grained analysis, we performed a series of independent samples t-tests across anatomical regions of the cerebellum to directly compare regional cerebellar volume (both GMV and WMV) and regional volumetric asymmetry in the two groups, applying Bonferroni correction using an alpha value of 0.05 (i.e. only $p < 0.001$ was considered

significant). Regions were extracted from the SUIT atlas (32 areas) (see Figure 2, Supplementary Table 2A and 2B).

We further hypothesized that cerebellar laterality would be different in healthy and chronic LH stroke group. To test this, we conducted a pair of two-tailed independent sample t-tests which revealed that both GMV LI and WMV LI were significantly different in the two groups ($t(491) = -11.25$, $p < 0.01$ and $t(491) = -6.44$, $p < 0.001$), indicating greater asymmetry favoring the left hemisphere in the chronic LH stroke group. These differences were widespread, including all but one sub-region of the cerebellum (Vermis Crus I, see figure 2).

In order to rule out the possibility that changes in cerebellar GMV observed in the stroke group were related solely to age, we examined the relationship between age and cerebellar volume in healthy adults. Consistent with the idea that brain volume generally decreases steadily after age 40 (Peters 2006), a Pearson correlation revealed that, within the healthy group, increased age was associated with decreased cerebellar GMV (p values < 0.001). Importantly, increasing age was not associated with changes in measures of volumetric asymmetry (i.e., LI GMV or the LI WMV, p values > 0.05), suggesting that the asymmetry observed in the chronic LH stroke group was likely unrelated to the normal aging process.

Based on the idea that changes in cerebellar GMV resulted from the cortical lesion itself, an assumption buttressed by the finding that changes in cerebellar asymmetry were not associated with aging per se (see above), we next examined correlations between lesion size, cerebellar volume and cerebellar asymmetry. Within the stroke group, a partial Pearson's correlation controlling for age, gender, and race revealed that lesion size in the left cortical hemisphere, was positively correlated with right cerebellar GMV, $r(236) = -0.21$, $p < 0.001$, but not with left cerebellar GMV ($p = 0.36$). Additionally, lesion size was positively correlated with both LI GMV, $r(239) = 0.379$, $p < 0.001$ and LI WMV, $r(239) = 0.22$, $p < 0.001$ values. Further, we explored the possibility that changes in cerebellar volume were related to time since stroke by conducting a Pearson correlation between cerebellar volume, asymmetry measures and days-post-stroke (at the time of the MRI scan). *Days-post-stroke* was positively correlated with both LI GMV, $r(239) = 0.19$, $p < 0.005$, and LI WMV, $r(239) = 0.12$, $p < 0.05$ scores, meaning that cerebellar volumetric imbalance increased as a function of time (**Table 2**). After controlling for lesion size, age, race and sex, a two-tailed partial correlation between days post-stroke and cerebellar GMV LI remained significant, $r(240) = 0.132$, $p = 0.042$, while the correlation with WMV LI was no longer significant, $r(240) = 0.155$, $p = 0.16$.

In general, there was a strong correlation between global measures of cerebellar GMV, LI GMV, and WAB-R scores. Notably a set of two planned Pearson correlations revealed that overall, left and right cerebellar GMV and WMV were positively correlated

with WAB_{TOTAL} scores (all p values < 0.001). Moreover, the positive correlation between cerebellar GMV and WMV and language ability was significant for each individual WAB-R sub-score (all p-values $\leqq 0.05$). Relationships between these variables that survived conditioning on age, sex, race, lesion size and days post stroke are shown in **Figure 3**.

In order to assess the value of adding region-specific cerebellar GMV to quantitative models of language ability (i.e. WAB_{TOTAL}), above and beyond other available metrics, we conducted a one-way ANOVA comparing two separate linear regression models. The first model used WAB_{TOTAL} as the dependent variable with demographic and cortical lesion characteristics as the independent variables, while the second model added cerebellar GMV values (one for each SUIT atlas ROI) as predictors. Addition of cerebellar GMV data to the model significantly improved fit, with an adjusted R^2 change from $H_0 = 0.41$, to $H_1 = 0.31$, 54 $F(34,76) = 7.15$, $p < 0.001$ (**Supplementary Table 4)**. Specific SUIT atlas regions in which greater cerebellar GMV was associated with improved scores included left VI (p = 0.025), right VIIa (p = 0.009), and vermis VIIb (p = 0.10). In order to further explore the value of adding cerebellar GMV data to models predicting specific linguistic abilities, we conducted a series of additional one-way ANOVAs as described above, this time treating each of the four WAB sub-scores {spontaneous speech, repetition, comprehension, naming} as the dependent variable. In all cases, addition of cerebellar GMV data to linear regression models significantly improved model fit (all p values < 0.001) above and beyond models that included only

demographic and cortical lesion data. These models identified a number of cerebellar regions in which higher GMV was associated with higher WAB-R sub-scores. Higher spontaneous speech sub-scores were associated with greater GMV in left I-IV ($p = 0.049$), Vermis VIIb (0.010) and right VIIIa ($p = 0.002$), right VIIIb ($p = 0.01$), higher naming sub-scores were associated with greater GMV in left VI ($p = 0.039$), right VIIIa ($p = 0.038$), and higher repetition sub-scores were associated with greater GMV in left VI ($p = 0.027$), Vermis VIIb ($p = 0.023$) and right VIIIa ($p = 0.006$). No regions emerged from the analysis of comprehension sub-scores (all p's < 0.08). Notably, both total GMV and GMV asymmetry were highly correlated with WAB_{TOTAL} scores ($r(232) = 0.21$, $p < 0.001$).

Finally, we assessed the value of adding region-specific cerebellar GMV data to regression models of treatment-related gains in picture naming ability. Specifically, we conducted a one-way ANOVA comparing two separate linear regression models using treatment-related gains as the dependent variable (i.e., difference in performance on a picture-cued object naming task compared both before and after treatment; see **Supplementary Methods**). As with the models described above, used to assess the relationship between WAB-R scores and region-specific cerebellar GMV, the first model was constrained to using demographic variables and lesion characteristics, whereas the second model additionally included region-specific cerebellar GMV data. Comparison of both models demonstrated that the model which included region-specific cerebellar

GMV values was significantly better than the model using demographic and cortical lesion measures alone (adjusted R^2 change from $H_0 = 0.15$ to $H_1 = 0.31$, $F(34,76) = 2.001$, $p = 0.016$, indicating that participants with greater cerebellar GMV experienced greater treatment gains). This effect was driven by cerebellar GMV differences in right cerebellar area Va ($p = 0.003$) (**Supplementary Table 4**).

Discussion

Cortical stroke is associated with both functional and structural changes at sites distal from the area of original infarct, and this diaschisis has been a primary focus of researchers and clinicians interested in predicting the severity of post-stroke sequelae as well as the likelihood of future recovery (Baldassarre et al., 2016; Kalinosky et al., 2017; Tang et al., 2016; Wilmskoetter et al., 2019, 2021). Cortical damage also impacts the cerebellum, via crossed cerebro-cortical connections, but less is known about the impact these changes have on stroke-related impairments. By examining cerebellar morphometry/asymmetry in individuals with aphasia as a consequence of chronic LH stroke, we were able to probe the relationship between cerebellar integrity (operationalized as gray matter volume and asymmetry), language ability and treatment response. This study is the first and largest to demonstrate clear and clinically meaningful changes in the contralateral cerebellar cortex in chronic LH stroke. We show that the inclusion of cerebellar gray matter volume and symmetry metrics significantly

improves models of language ability (WAB-R scores) and improvement trajectory (changes in picture naming), above and beyond models based on demographic and cortical lesion-related predictors alone.

Cortical Lesion Characteristics and Cerebellar GMV Changes

Within our chronic LH stroke cohort, we observed a strong positive correlation between lesion size and changes in cerebellar GMV and laterality. Notably, these changes were not present in a healthy cohort, even after controlling for demographic factors such as age, gender and race, suggesting that the observed changes were not simply the product of age-related CNS atrophy. We also found that cerebellar imbalance, operationalized as asymmetry between left and right cerebellar GMV, was positively correlated with days post stroke, a finding that held true even when controlling for demographic factors (age, race, sex) and lesion size. This finding raises the possibility that changes in cerebellar volume may still occur well into the chronic stages of stroke, a possibility which has not previously been considered. While more research is clearly necessary both to confirm this, and, if confirmed, to fully delineate the time-course of cerebellar GMV changes following stroke, the possibility that such changes may occur over a period of years could have profound implications for aphasia treatment. Most importantly, exploring this relationship could help to define the therapeutic time window during which potentially ameliorative/preventative adjuvant therapies are maximally beneficial.

Cerebellar GMV Changes in Chronic LH Stroke

A striking aspect of this study is the highly significant and widespread nature of the changes in cerebellar GMV and GM symmetry observed in individuals with chronic LH stroke. Compared to healthy adults, individuals with chronic LH stroke showed significantly lower cerebellar GMV in both the left and right cerebellar hemispheres, and this difference was particularly apparent within right cerebellar GM. The significant differences in the laterality of cerebellar gray matter volume in individuals with chronic LH stroke, argues against concern that changes in cerebellar GMV are simply the result of age-related global CNS atrophy. This finding is not particularly surprising, given prior research describing structural connectivity between the left cerebral hemisphere and the right cerebellum (Diedrichsen et al., 2009; Jansen et al., 2005; Moberget & Ivry, 2016).

The most parsimonious explanation for reductions in cerebellar GMV observed in the chronic LH group in the current study is that it resulted from the process of Wallerian (anterograde) degeneration, a process that occurs when cerebellar cell density is decreased following removal of input from cortical cells. Based on what is known about this process, downstream effects on the cerebellum GMV would be expected to evolve over the course of weeks or months. For example, necrosis of cortical neurons, caused by stroke-related hypoperfusion or hemorrhage, typically takes place within a timeframe

of days to weeks, with survival of perilesional neurons likely varying as a function of their distance from the primary lesion site (Brown 2021) . Following death of these cortical cells, the survival of contralateral cerebellar cells denied their input would likely depend on several factors, including the number of connections removed, remaining connectivity and time since injury, all of which are difficult to measure, but would likely evolve across weeks as well (Fink and Cookson 2005). One intriguing possibility is changes in the cortex result in changes within the cerebellum which, in turn result in further cortical changes. The existence of this decidedly 'vicious cycle', could continue to alter brain structure for months or even years after stroke is certainly plausible. Indeed, there is already evidence that stroke lesions continue to expand years after stroke (Seghier et al. 2014). However, it is also clear that more research must be done to chart the exact time-course of this process and the exact mechanisms supporting these degenerative cerebro-cortical effects.

Aphasia Severity and Cerebellar GMV in Chronic LH Stroke

An important finding of the current study is that cerebellar gray matter volume and asymmetry have clinical significance. Cerebellar GMV, WMV (left hemisphere, right hemisphere, and total volume) and asymmetry were positively correlated with each of the WAB-R sub-scores (spontaneous speech, repetition, naming and comprehension). These broad measures of cerebellar health were significant predictors of WAB-R scores even after controlling for demographic (age, race, sex) and cortical putative lesion-

based measures (lesion size, days post-stroke), traditionally thought to account for the vast majority of variability in chronic stroke aphasia severity and treatment outcomes (Schiemanck et al., 2005) (Figure 3).

Regression models of both aphasia severity (as measured by the WAB-R) and treatment recovery (as measured by improvements in picture-cued object naming) benefitted from inclusion of cerebellar GMV data. Using a region-of-interest (ROI) based analysis in which the cerebellum was divided into 34 spatially distinct areas, we demonstrate that regional cerebellar GMV explains unique variability in both aphasia severity and treatment trajectories, significantly improving models based on other known factors. This finding was also illustrated in a prior meta-analysis identifying cerebellar areas Crus I, Crus II as well as Lobules VI and VIIA (Mariën and Manto 2015). Our results, which identify a number of specific cerebellar ROIs in which WAB-R and sub-scores were significantly correlated with higher cerebellar GMV including left 1-IV, left VI, right VIIIa, right VIIIb and Vermis VIIb partially overlap with these findings. For example, our data indicated that higher cerebellar GMV in left area VI was associated with higher WAB-R_{TOTAL} scores as well as higher scores on the repetition and naming WAB-R sub-scores. Interestingly, we also found an association between WAB-R spontaneous speech scores and GMV in two areas that have been linked to working memory, namely left area I-IV (Guell et al. 2018) and right area VIIIa (Stoodley and Schmahmann 2009; Stoodley 2014). This makes sense given the fact that working

memory is known to be important for retrieval of words and construction of more complex, multi-word utterances (Deldar et al. 2021; Baddeley 2003). Although not identified in the meta-analysis by Marien et al., right cerebellar regions VIIb and VIIIa have been linked to linguistic functions by other researchers (Stoodley and Schmahmann 2009), with area VIIb showing increased fMRI signal during a verb generation task (Stoodley et al. 2012), and one study reported higher cerebellar volumes in cerebellum area VIIIa was linked to higher language abilities in children with autism spectrum disorder (Hodge et al. 2010).

Aphasia Treatment Response and Cerebellar GMV in Chronic LH Stroke

An important finding in the current study was that inclusion of GMV in linear regression models of treatment response significantly improved model fit, increasing variance from R2 = 0.21 to R2 = 0.62, a change of 0.41, with a calculated effect size of 1.62, Cohen's f2 = R2/1-R2/(DF_{MODEL}-$DF_{RESIDUAL}$). Cerebellar GMV within right area V was the most significant predictor in this model. Right cerebellar area V has been implicated in both working memory and emotional processing. Taken together with findings described above which also implicate working memory related areas in aphasia severity, this finding provides compelling converging evidence that working memory is a key factor in treatment response in chronic LH aphasia. This meshes well with prior work investigating working memory and language ability in aphasia. For example, according to a study by Lee and Pyun (Lee and Pyun 2014), attention and working

memory were significantly impaired in aphasic patients compared to controls. In another study, aphasia severity and working memory impairments were highly correlated (Yu et al. 2013). There is also some evidence that treatments designed to rehabilitate short-term and working memory can improve language function following aphasia (Martin et al. 2021; Majerus 2018).

One of the main clinical payoffs of precisely localizing cerebellar changes associated with language and stroke is that such findings can inform targeting procedures of brain-stimulation based treatments. Indeed, the impact of cerebellar stimulation, specifically transcranial direct current stimulation, has already been investigated within the field of stroke, with some initial studies showing that application of deep brain stimulation and transcranial direct current stimulation (tDCS) to the cerebellum can improve recovery in both animal and human models, possibly by enhancing the excitability of surviving cortical neurons (Machado and Baker 2012; Sebastian et al., 2016; van Dun & Manto, 2018). Critically, both the optimal timing of brain-stimulation based approaches, as well as the exact dosages needed to maximize recovery remain unknown. These factors will have to be considered in relation to the evolution of cortical and cerebellar changes following stroke, which is temporally complex, and likely evolves in ways that are not currently well understood. Both downstream and upstream pathways need to be considered based on the known relationship between cerebral and cerebellar function (i.e. although beyond the scope of this paper, extant literature suggests that, in addition

to cerebellar stimulation, cortical stimulation may positively impact recovery from aphasia following stroke) (Ashaie et al. 2022). The optimization of stimulation location and treatment timing presents a clear avenue for future research and an important opportunity for collaboration between clinicians and researchers working with both acute and chronic stroke populations.

The interpretation of this study is necessarily subject to certain limitations. First, the current sample was limited to a relatively homogeneous cohort of individuals with LH stroke with aphasia, making it uncertain whether or not the patterns identified here will hold for other types of stroke or stroke-related sequalae. Second, ROI-related overlap between findings from the present study and prior investigations of the relationship between language and the cerebellum (using healthy or other clinical populations) should be interpreted with caution given the known potential for neural reorganization following stroke. An additional limitation, albeit one that presents a tantalizing opportunity for future investigation, is that the present study did not attempt to relate specific patterns of cortical damage to specific patterns of change in cerebellar GMV or laterality. Cortical models of aphasia severity and recovery that account for the spatial distribution of the lesion, in addition to lesion size, are generally superior (Park et al. 2016; Sul et al. 2019; Forkel and Catani 2018; Fridriksson 2010). If spatial characteristics of cortical lesions are meaningfully related to changes observed in the

cerebellum, then it may be possible to further improve the fit of predictive models of aphasia severity and/or treatment response by combining these data.

General Conclusion

The current study highlights the importance of cerebellar integrity in individuals with chronic LH stroke and aphasia. By identifying differences in cerebellar GVM in healthy individuals and individuals with stroke, this study demonstrates that cortical stroke has a significant impact on cerebellar volume and symmetry. An attempt to understand the implications of these novel findings also raises interesting new questions about the nature of neural changes following stroke. For example, what is the time-window over which cortical and cerebellar changes occur, how are cortical and cerebellar changes linked together [do they reverberate], what is the relationship between spatial characteristics of cortical lesions and spatial properties of cerebellar GMV changes, and, finally, how can we use the answers to all of these questions to inform the design of better brain-stimulation based treatment interventions for chronic LH stroke and aphasia, or any other type of stroke and subsequent sequelae for that matter? Clearly, these questions would best be answered by a comprehensive longitudinal research program in which experts in acute and chronic stroke collaborate to investigate cerebral and cerebellar changes as they evolve across time. In the end, pursuit of such research promises plenty of potential gains for researchers interested in brain plasticity, clinicians

interested in improving aphasia-related impairments, and patients dedicated to recovery and discovery.

References

Baldassarre, A., Ramsey, L. E., Siegel, J. S., Shulman, G. L., & Corbetta, M. (2016). Brain connectivity and neurological disorders after stroke. In *Current Opinion in Neurology* (Vol. 29, Issue 6, pp. 706–713). https://doi.org/10.1097/wco.0000000000000396

Basilakos, A., Stark, B. C., Johnson, L., Rorden, C., Yourganov, G., Bonilha, L., & Fridriksson, J. (2019). Leukoaraiosis Is Associated With a Decline in Language Abilities in Chronic Aphasia. *Neurorehabilitation and Neural Repair*, *33*(9), 718–729.

DeMarco, A. T., Dvorak, E., Lacey, E., Stoodley, C. J., & Turkeltaub, P. E. (2021). An Exploratory Study of Cerebellar Transcranial Direct Current Stimulation in Individuals With Chronic Stroke Aphasia. *Cognitive and Behavioral Neurology: Official Journal of the Society for Behavioral and Cognitive Neurology*, *34*(2), 96–106.

Desmond, J. E., & Fiez, J. A. (1998). Neuroimaging studies of the cerebellum: language, learning and memory. In *Trends in Cognitive Sciences* (Vol. 2, Issue 9, pp. 355–362). https://doi.org/10.1016/s1364-6613(98)01211-x

Diedrichsen, J., Balsters, J. H., Flavell, J., Cussans, E., & Ramnani, N. (2009). A probabilistic MR atlas of the human cerebellum. *NeuroImage*, *46*(1), 39–46.

Fiez, J. A. (2016). The cerebellum and language: Persistent themes and findings. *Brain and Language*, *161*, 1–3.

Fridriksson, J., Baker, J. M., & Moser, D. (2009). Cortical mapping of naming errors in aphasia. *Human Brain Mapping*, *30*(8), 2487–2498.

Gaser, C., Dahnke, R., Thompson, P. M., Kurth, F., Luders, E., & Alzheimer's Disease Neuroimaging Initiative. (n.d.). *CAT – A Computational Anatomy Toolbox for the Analysis of Structural MRI Data*. https://doi.org/10.1101/2022.06.11.495736

Heart and Stroke Association Statistics. (n.d.). Retrieved December 8, 2020, from https://www.heart.org/en/about-us/heart-and-stroke-association-statistics

Jansen, A., Flöel, A., Van Randenborgh, J., Konrad, C., Rotte, M., Förster, A.-F., Deppe, M., & Knecht, S. (2005). Crossed cerebro-cerebellar language dominance. *Human Brain Mapping*, *24*(3), 165–172.

Justus, T. (2004). The cerebellum and English grammatical morphology: evidence from production, comprehension, and grammaticality judgments. *Journal of Cognitive Neuroscience*, *16*(7), 1115–1130.

Kalinosky, B. T., Barillas, R. B., & Schmit, B. D. (2017). Structurofunctional resting-state networks correlate with motor function in chronic stroke. In *NeuroImage: Clinical* (Vol. 16, pp. 610–623). https://doi.org/10.1016/j.nicl.2017.07.002

Kertesz, A. (2022). The Western Aphasia Battery: a systematic review of research and clinical applications. In *Aphasiology* (Vol. 36, Issue 1, pp. 21–50). https://doi.org/10.1080/02687038.2020.1852002

Lanska, D. J., & Kuller, L. H. (1995). The geography of stroke mortality in the United States and the concept of a stroke belt. *Stroke; a Journal of Cerebral Circulation*,

26(7), 1145–1149.

Laska, A. C., Hellblom, A., Murray, V., Kahan, T., & Von Arbin, M. (2001). Aphasia in acute stroke and relation to outcome. *Journal of Internal Medicine*, *249*(5), 413–422.

Leiner, H. C., Leiner, A. L., & Dow, R. S. (1993). Cognitive and language functions of the human cerebellum. In *Trends in Neurosciences* (Vol. 16, Issue 11, pp. 444–447). https://doi.org/10.1016/0166-2236(93)90072-t

Machado, A., & Baker, K. B. (2012). Upside down crossed cerebellar diaschisis: proposing chronic stimulation of the dentatothalamocortical pathway for post-stroke motor recovery. *Frontiers in Integrative Neuroscience*, *6*, 20.

Moberget, T., & Ivry, R. B. (2016). Cerebellar contributions to motor control and language comprehension: searching for common computational principles. In *Annals of the New York Academy of Sciences* (Vol. 1369, Issue 1, pp. 154–171). https://doi.org/10.1111/nyas.13094

Nachev, P., Coulthard, E., Jäger, H. R., Kennard, C., & Husain, M. (2008). Enantiomorphic normalization of focally lesioned brains. *NeuroImage*, *39*(3), 1215–1226.

Newman-Norlund, R.D., Newman-Norlund, S.E., Sayers, S., Nemati, S., Riccardi, N., Rorden, C., Fridriksson, J. (2021). The Aging Brain Cohort (ABC) repository: The University of South Carolina's multimodal lifespan database for studying the relationship between the brain, cognition, genetics and behavior in healthy aging.

NeuroImage Reports.

Penny, W. D., Friston, K. J., Ashburner, J. T., Kiebel, S. J., & Nichols, T. E. (2011). *Statistical Parametric Mapping: The Analysis of Functional Brain Images*. Elsevier.

Rorden, C., Fridriksson, J., & Karnath, H.-O. (2009). An evaluation of traditional and novel tools for lesion behavior mapping [Review of *An evaluation of traditional and novel tools for lesion behavior mapping*]. *NeuroImage*, *44*(4), 1355–1362.

Rorden, C., McKinnon, E., Hanayik, T., Yourganov, G., Newman-Norlund, R. D., & Reddy, D. P. (2020). *rogiedodgie/nii_preprocess: Zenodo DOI release*. https://doi.org/10.5281/zenodo.4027711

Schiemanck, S. K., Post, M. W. M., Witkamp, T. D., Kappelle, L. J., & Prevo, A. J. H. (2005). Relationship between ischemic lesion volume and functional status in the 2nd week after middle cerebral artery stroke. *Neurorehabilitation and Neural Repair*, *19*(2), 133–138.

Sebastian, R., Saxena, S., Tsapkini, K., Faria, A. V., Long, C., Wright, A., Davis, C., Tippett, D. C., Mourdoukoutas, A. P., Bikson, M., Celnik, P., & Hillis, A. E. (2016). Cerebellar tDCS: A Novel Approach to Augment Language Treatment Post-stroke. *Frontiers in Human Neuroscience*, *10*, 695.

Seghier, M. L. (2008). Laterality index in functional MRI: methodological issues. *Magnetic Resonance Imaging*, *26*(5), 594–601.

Silveri, M. C., Leggio, M. G., & Molinari, M. (1994). The cerebellum contributes to linguistic production. In *Neurology* (Vol. 44, Issue 11, pp. 2047–2047).

https://doi.org/10.1212/wnl.44.11.2047

Suarez, A., Saxena, S., Oishi, K., Oishi, K., Walker, A., Rorden, C., & Hillis, A. E. (2020). Influence of age, lesion volume, and damage to dorsal versus ventral streams to viewer- and stimulus-centered hemispatial neglect in acute right hemisphere stroke. In *Cortex* (Vol. 126, pp. 73–82). https://doi.org/10.1016/j.cortex.2019.12.030

Tang, C., Zhao, Z., Chen, C., Zheng, X., Sun, F., Zhang, X., Tian, J., Fan, M., Wu, Y., & Jia, J. (2016). Decreased Functional Connectivity of Homotopic Brain Regions in Chronic Stroke Patients: A Resting State fMRI Study. *PloS One*, *11*(4), e0152875.

van Dun, K., & Manto, M. (2018). Non-invasive Cerebellar Stimulation: Moving Towards Clinical Applications for Cerebellar and Extra-Cerebellar Disorders. *Cerebellum* , *17*(3), 259–263.

van Niftrik, C. H. B., Visser, T. F., Sebök, M., Muscas, G., El Amki, M., Serra, C., Regli, L., Wegener, S., & Fierstra, J. (2021). Delayed cerebral atrophy after cerebellar stroke: topographical relation and clinical impact. *Brain Communications*, *3*(4), fcab279.

Whitwell, J. L., Crum, W. R., Watt, H. C., & Fox, N. C. (2001). Normalization of cerebral volumes by use of intracranial volume: implications for longitudinal quantitative MR imaging. *AJNR. American Journal of Neuroradiology*, *22*(8), 1483–1489.

Wilmskoetter, J., Fridriksson, J., Basilakos, A., Phillip Johnson, L., Marebwa, B., Rorden, C., Warner, G., Hickok, G., Hillis, A. E., & Bonilha, L. (2021). Indirect White

Matter Pathways Are Associated With Treated Naming Improvement in Aphasia. *Neurorehabilitation and Neural Repair*, *35*(4), 346–355.

Wilmskoetter, J., Marebwa, B., Basilakos, A., Fridriksson, J., Rorden, C., Stark, B. C., Johnson, L., Hickok, G., Hillis, A. E., & Bonilha, L. (2019). Long-range fibre damage in small vessel brain disease affects aphasia severity. *Brain: A Journal of Neurology*, *142*(10), 3190–3201.

Yourganov, G., Fridriksson, J., Stark, B., & Rorden, C. (2018). Removal of artifacts from resting-state fMRI data in stroke. *NeuroImage. Clinical*, *17*, 297–305.

Yourganov, G., Smith, K. G., Fridriksson, J., & Rorden, C. (2015). Predicting aphasia type from brain damage measured with structural MRI. *Cortex; a Journal Devoted to the Study of the Nervous System and Behavior*, *73*, 203–215.

Zettin, M., Cappa, S. F., D'amico, A., Rago, R., Perino, C., Perani, D., & Fazio, F. (1997). Agrammatic speech production after a right cerebellar haemorrhage. In *Neurocase* (Vol. 3, Issue 5, pp. 375–380). https://doi.org/10.1080/13554799708411976

Table 1. Control and Chronic Stroke Population Demographics. **M** = mean, **SD** = standard deviation. Comma-delimited numbers in parentheses denote minimum and maximum values for each variable.

	Chronic Stroke (N=249)	**Healthy Controls (N=244)**
Age (yrs)	M = 60.5, **SD** = 11.4 (29,81)	**M** = 45.8, **SD** = 11.4 (20,79)
Gender	Female = 153 (61%) Male = 96 (39%)	Female = 185 (76%) Male = 59 (24%)
Race	White = 208 (84%) Black = 39 (15%) Other = (1%)	White = 208 (85%) Black = 25 (10%) Other = 11 (5%)
Lesion Size (cm3)	**M** =118.3, **SD** =96.6 (1.5,479.2)	N/A
Time Post Stroke (days)	M = 1639, **SD** = 1672 (205, 9301)	N/A

Figure 1. Cerebellar volume in chronic LH stroke with aphasia and controls after accounting for age, race and gender. Cerebellar volume was significantly lower in chronic LH stroke with aphasia and controls in *all areas shown (*right WMV, p = 0.32, all other areas p < 0.001). *Error bars represent standard deviation...

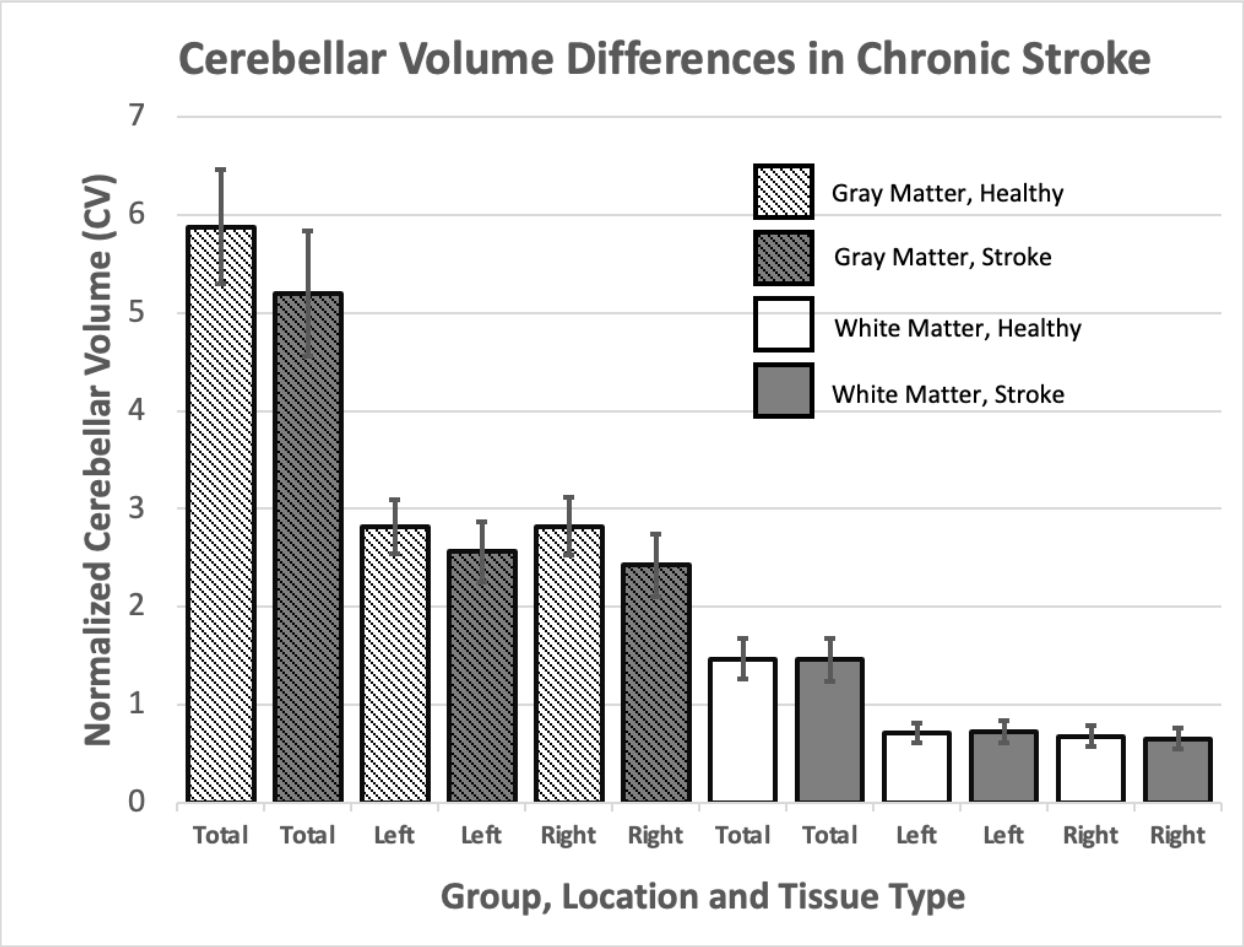

Figure 2. Spatial locations of significant differences in cerebellar volume (controls vs chronic LH stroke) on a flat-map of the cerebellum created using the SUIT processing suite. Values in **colorbar** represent spmT values from a direct comparison (independent samples t-test) of cerebellar GMV maps created for each group by SUIT. Differences in cerebellar GMV were most pronounced in the right hemisphere of the cerebellum for chronic LH stroke. These effects were evident across the majority of cerebellar regions (see **Supplementary Table 2A**).

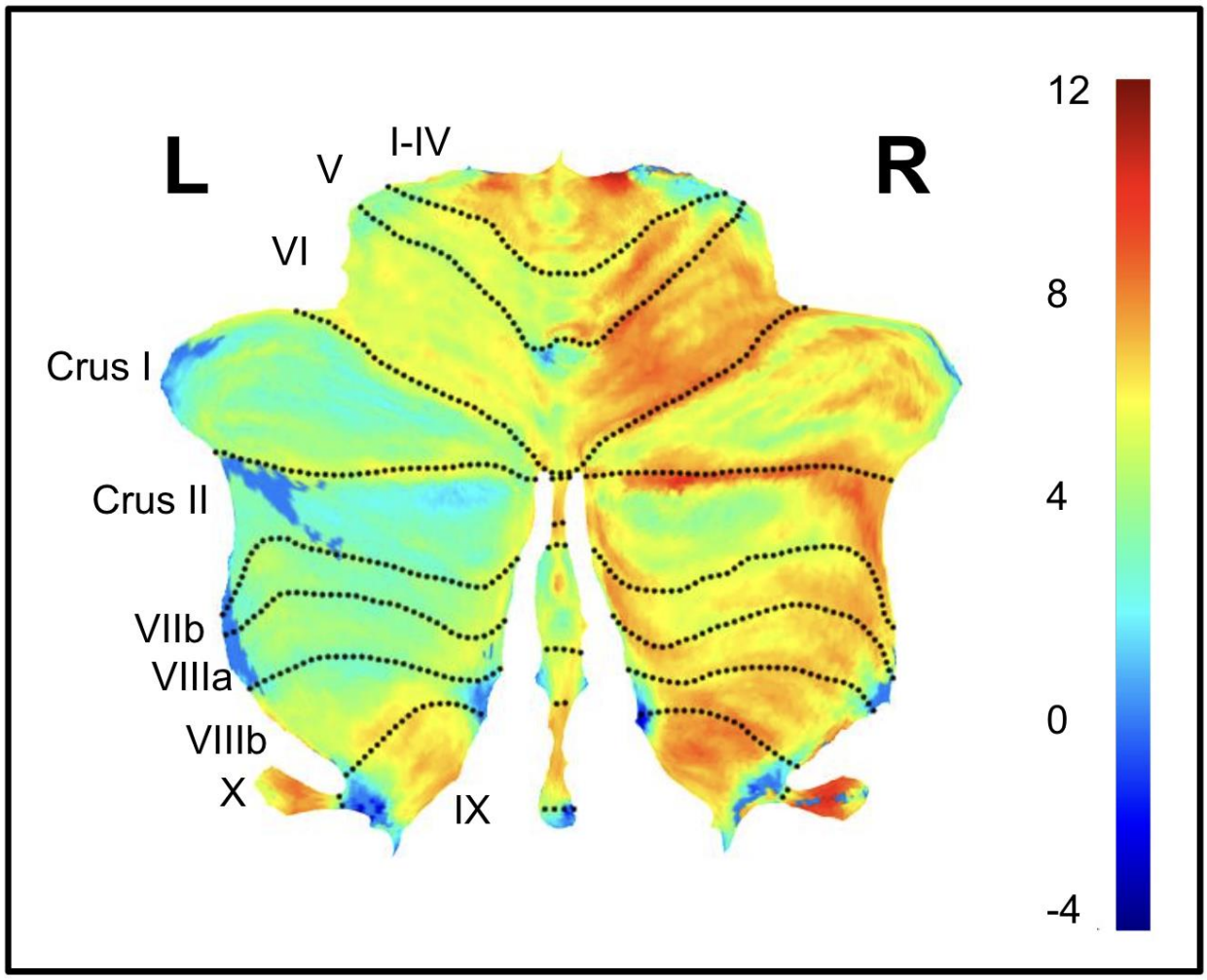

Figure 3. One-sample partial Pearson and partial distance (i.e., nonlinear) correlations between WAB scores (rows) and cerebellar volume / symmetry indices (columns) after conditioning on age, sex, race, lesion size and days since stroke. Red text above each scatterplot highlights relationships significant for both types of correlations ($p < 0.05$). Black text indicates relationship insignificance for both types of correlations. Blue text indicates significant nonlinear relationship and insignificant linear relationship. Green text indicates significant linear relationship and insignificant nonlinear relationship. **r^2** = Partial Pearson correlation coefficient squared (i.e., explained variance), **DC** = Distance Correlation coefficient,**GVM** = gray matter volume, **WMV** = white matter volume, **WAB** = Western Aphasia battery, **Spontaneous** = spontaneous speech subscore, **Comp** = comprehension subscore, **Repetition** = repetition subscore, **Naming** = naming subscore.

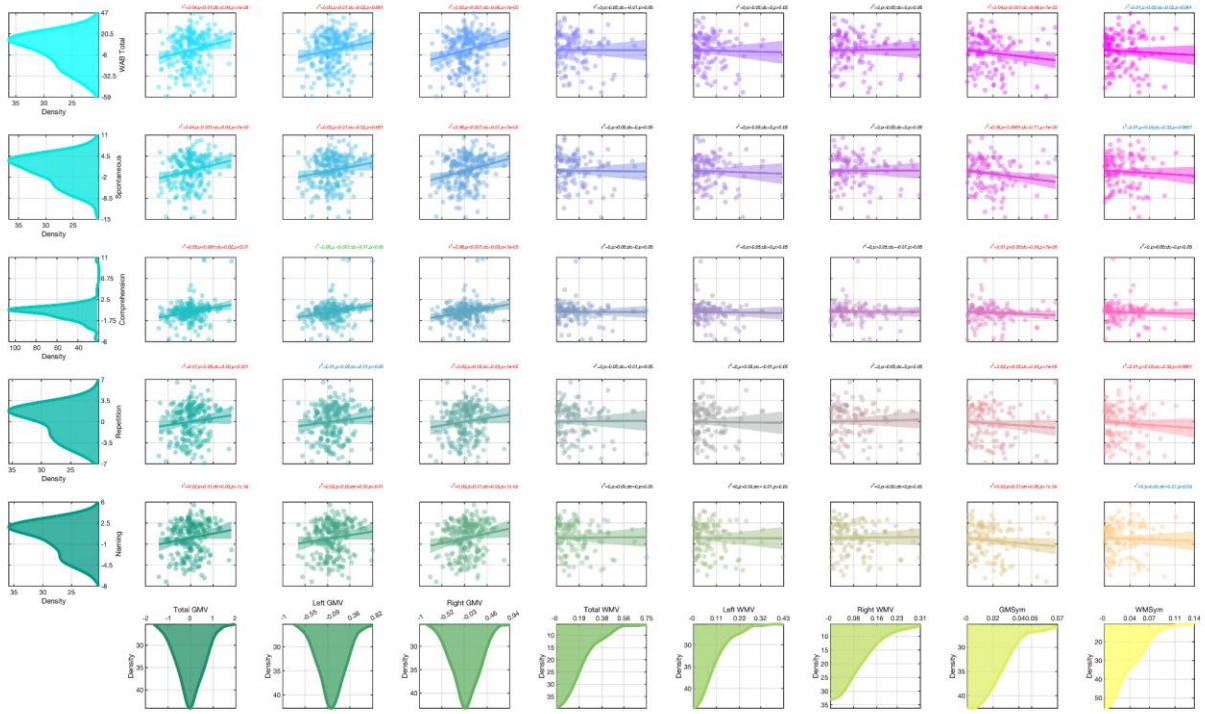

Figure 4. Within our sample of chronic LH stroke, a number of participants took part in aphasia treatment studies (N = 77) involving both phonological and semantic training We found that right cerebellar GMV accounted for significant additional variability in treatment gains, as defined by changes in *Treated40* (i.e. improvement in ability to name visually cued objects) scores. Cerebellar GMV was predictive of improvements even after accounting for demographic (age, race, gender) and cortical lesion (lesion

size and days post stroke) characteristics.

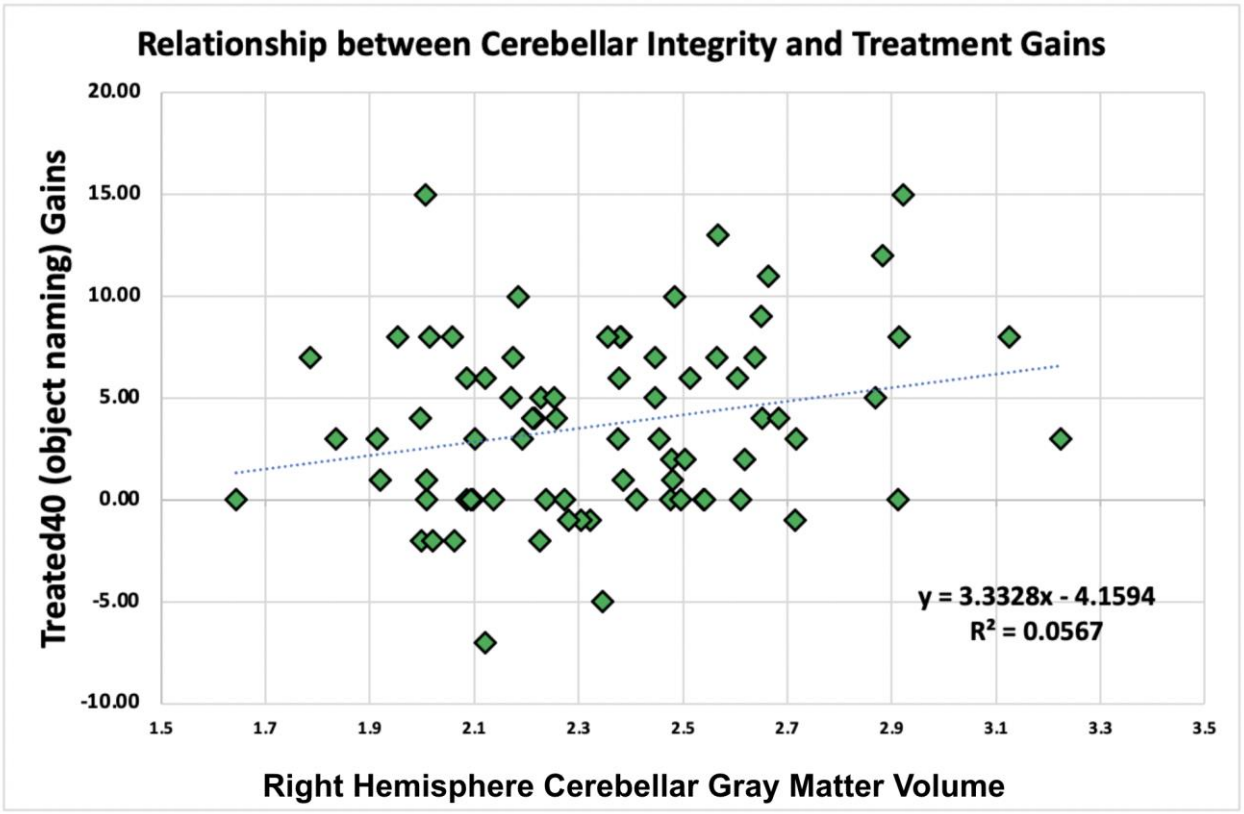

Supplementary Table 1A. Correlations between demographic factors and cerebellar volume in healthy adult participants. Correlations where 0.12 < r > -0.12, are significant at $p < 0.05$.

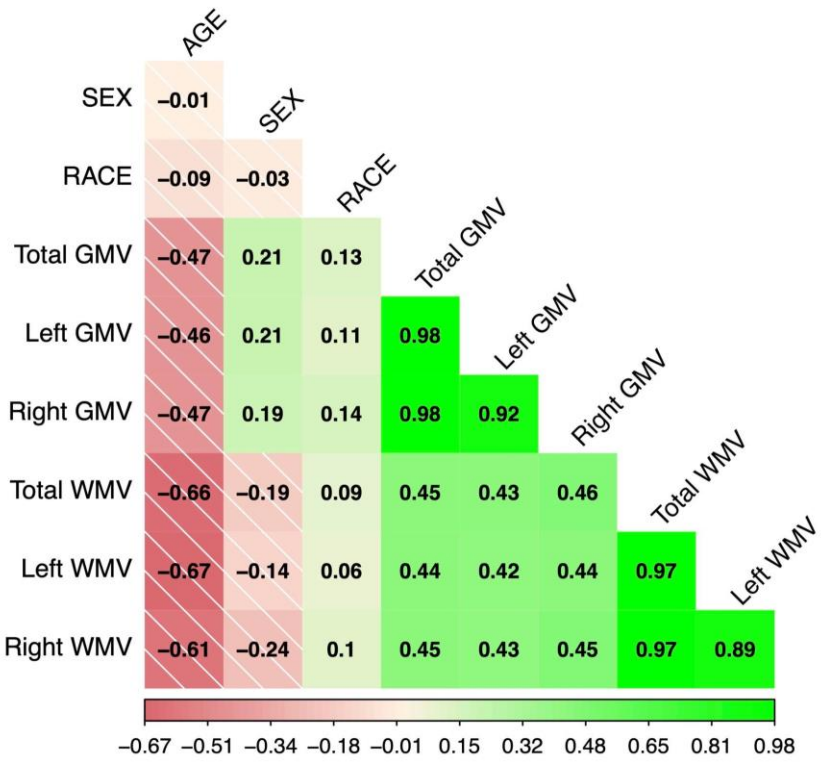

Supplementary Table 1B. Correlations between demographic factors and cerebellar volume individuals with chronic LH stroke. Correlations where 0.12 < r > -0.12, are significant at p < 0.05.

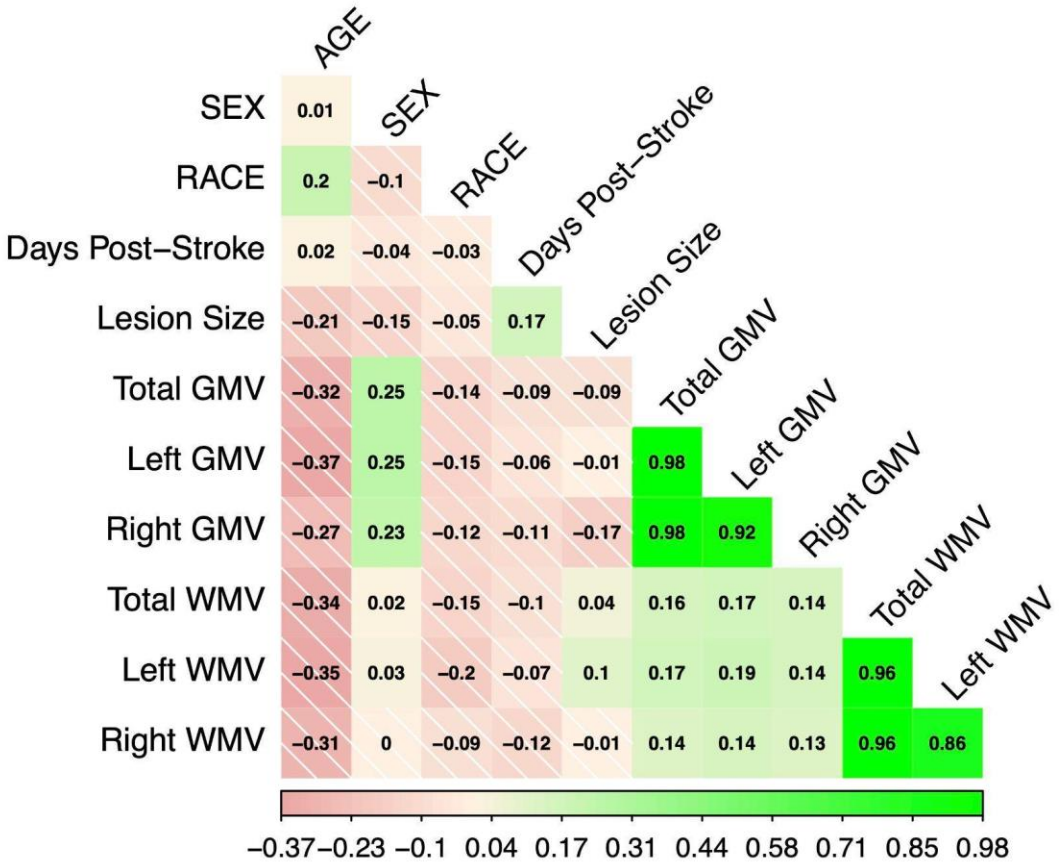

Supplementary Table 2A. Differences in cerebellar GMV in healthy and stroke groups, shown separately for each individual cerebellar **GM** region in the SUIT atlas, after

controlling for differences in age, race and gender.

Area	type	N	Mean	min	max	stDev	SEM	t	df	p-value	effect size
Left_I-IV	heathy	244	0.1308	0.085	0.089	0.015	0.0009	6.122	491	<.001	0.546
	stroke	249	0.1218	0.119	0.0789	0.018	0.0011				
Right_I-IV	heathy	244	0.1559	0.096	0.1084	0.018	0.0011	7.717	491	<.001	0.688
	stroke	249	0.1426	0.121	0.0959	0.021	0.0013				
Left_V	heathy	244	0.1918	0.12	0.131	0.02	0.0013	8.447	491	<.001	0.753
	stroke	249	0.1764	0.124	0.1219	0.021	0.0013				
Right_V	heathy	244	0.2023	0.164	0.1081	0.023	0.0014	13.303	491	<.001	1.186
	stroke	249	0.1744	0.126	0.1218	0.024	0.0015				
Left_VI	heathy	244	0.4558	0.379	0.208	0.053	0.0033	12.026	491	<.001	1.072
	stroke	249	0.3994	0.306	0.2676	0.052	0.0033				
Vermis_VI	heathy	244	0.0793	0.054	0.0558	0.01	0.0006	7.225	491	<.001	0.644
	stroke	249	0.073	0.06	0.0508	0.01	0.0007				
Right_VI	heathy	244	0.4308	0.414	0.1581	0.051	0.0032	16.08	491	<.001	1.434
	stroke	249	0.3574	0.261	0.25	0.051	0.0032				
Left_CrusI	heathy	244	0.6593	0.466	0.3994	0.081	0.0051	9.323	491	<.001	0.831
	stroke	249	0.5918	0.499	0.3805	0.082	0.0051				
Vermis_CrusI	heathy	244	0.0006	0.002	0	3E-04	0	0.897	491	0.37	0.08
	stroke	249	0.0006	0.002	0	3E-04	0				
Right_CrusI	heathy	244	0.6399	0.625	0.2078	0.081	0.0051	12.077	491	<.001	1.077
	stroke	249	0.5519	0.516	0.3304	0.082	0.0052				
Left_CrusII	heathy	244	0.4895	0.346	0.3127	0.06	0.0038	6.878	491	<.001	0.613
	stroke	249	0.4514	0.367	0.3069	0.064	0.004				
Vermis_CrusII	heathy	244	0.0191	0.016	0.0103	0.003	0.0002	4.622	491	<.001	0.412
	stroke	249	0.018	0.016	0.0114	0.003	0.0002				
Right_CrusII	heathy	244	0.482	0.534	0.1903	0.063	0.004	12.13	491	<.001	1.082
	stroke	249	0.411	0.379	0.2303	0.068	0.0043				
Left_VIIb	heathy	244	0.2734	0.204	0.1797	0.034	0.0021	6.557	491	<.001	0.585
	stroke	249	0.2519	0.201	0.1644	0.039	0.0025				
Vermis_VIIb	heathy	244	0.0096	0.012	0.0047	0.002	0.0001	11.461	491	<.001	1.022
	stroke	249	0.0079	0.01	0.0043	0.002	0.0001				
Right_VIIb	heathy	244	0.2739	0.299	0.0969	0.036	0.0023	12.962	491	<.001	1.156
	stroke	249	0.2304	0.255	0.1186	0.039	0.0025				
Left_VIIIa	heathy	244	0.2602	0.26	0.1124	0.03	0.0019	6.554	491	<.001	0.584
	stroke	249	0.2414	0.181	0.1621	0.035	0.0022				
Vermis_VIIIa	heathy	244	0.0494	0.035	0.0305	0.006	0.0004	7.298	491	<.001	0.651
	stroke	249	0.0452	0.046	0.0234	0.007	0.0004				
Right_VIIIa	heathy	244	0.2534	0.245	0.0915	0.03	0.0019	12.427	491	<.001	1.108
	stroke	249	0.2168	0.229	0.1364	0.036	0.0022				
Left_VIIIb	heathy	244	0.1908	0.188	0.0826	0.025	0.0015	4.871	491	<.001	0.434
	stroke	249	0.1796	0.167	0.1054	0.027	0.0017				
Vermis_VIIIb	heathy	244	0.0274	0.023	0.0156	0.004	0.0003	7.013	491	<.001	0.625
	stroke	249	0.0248	0.029	0.0152	0.004	0.0003				
Right_VIIIb	heathy	244	0.1964	0.18	0.0918	0.025	0.0016	10.016	491	<.001	0.893
	stroke	249	0.1729	0.184	0.0844	0.028	0.0017				
Left_IX	heathy	244	0.1373	0.132	0.0736	0.023	0.0014	7.119	491	<.001	0.635
	stroke	249	0.1224	0.124	0.0732	0.024	0.0015				
Vermis_IX	heathy	244	0.0341	0.03	0.02	0.006	0.0004	7.707	491	<.001	0.687
	stroke	249	0.03	0.037	0.0139	0.006	0.0004				
Right_IX	heathy	244	0.1557	0.15	0.0728	0.023	0.0015	9.441	491	<.001	0.842
	stroke	249	0.1351	0.133	0.0758	0.025	0.0016				
Left_X	heathy	244	0.0269	0.024	0.0123	0.004	0.0002	3.871	491	<.001	0.345
	stroke	249	0.0256	0.023	0.0154	0.004	0.0003				
Vermis_X	heathy	244	0.0145	0.014	0.0081	0.002	0.0002	6.924	491	<.001	0.617
	stroke	249	0.013	0.016	0.0081	0.002	0.0002				
Right_X	heathy	244	0.0292	0.022	0.0182	0.004	0.0002	4.762	491	<.001	0.425
	stroke	249	0.0275	0.023	0.0186	0.004	0.0003				
Left_Total	heathy	244	2.8158	1.928	1.8104	0.281	0.0177	9.717	491	<.001	0.866
	stroke	249	2.5617	1.643	1.807	0.305	0.0192				
Right_Total	heathy	244	2.8193	2.556	1.159	0.298	0.0188	14.565	491	<.001	1.299
	stroke	249	2.4201	1.717	1.6429	0.317	0.02				
GMV LI	heathy	244	-2E-04	0.507	-0.106	0.028	0.0018	-11.35	491	<.001	-1.012
	stroke	249	0.0274	0.17	-0.046	0.026	0.0017				

Supplementary Table 2B. Differences in cerebellar WMV in healthy and stroke groups, shown separately for each individual cerebellar **WM** region in the SUIT atlas,

after controlling for differences in age, race and gender.

	type	N	Mean	min	max	stDev	SEM	t	df	p-value	effect size
Left_I-IV	heathy	244	0.0522	0.039	0.0318	0.007	0.0004	-0.708	491	0.479	-0.063
	stroke	249	0.0527	0.055	0.0275	0.008	0.0005				
Right_I-IV	heathy	244	0.0562	0.051	0.0314	0.008	0.0005	4.96	491	<.001	0.442
	stroke	249	0.0525	0.058	0.0273	0.009	0.0005				
Left_V	heathy	244	0.0701	0.05	0.048	0.009	0.0006	-2.375	491	0.018	-0.212
	stroke	249	0.0723	0.066	0.0387	0.011	0.0007				
Right_V	heathy	244	0.054	0.045	0.0342	0.009	0.0006	0.683	491	0.495	0.061
	stroke	249	0.0534	0.056	0.0263	0.01	0.0006				
Left_VI	heathy	244	0.125	0.122	0.074	0.023	0.0014	-4.819	491	<.001	-0.43
	stroke	249	0.1354	0.147	0.0799	0.026	0.0016				
Vermis_VI	heathy	244	0.025	0.027	0.0135	0.005	0.0003	4.35	491	<.001	0.388
	stroke	249	0.0231	0.03	0.0089	0.005	0.0003				
Right_VI	heathy	244	0.0953	0.141	0.0254	0.021	0.0013	-0.91	491	0.363	-0.081
	stroke	249	0.0971	0.123	0.0445	0.023	0.0015				
Left_CrusI	heathy	244	0.1446	0.207	0.0849	0.029	0.0018	1.05	491	0.294	0.094
	stroke	249	0.1418	0.218	0.0796	0.031	0.0019				
Vermis_CrusI	heathy	244	0	4E-04	0	1E-04	0	0.495	491	0.621	0.044
	stroke	249	0	5E-04	0	1E-04	0				
Right_CrusI	heathy	244	0.1531	0.237	0.0261	0.033	0.0021	4.086	491	<.001	0.364
	stroke	249	0.1414	0.193	0.0765	0.031	0.002				
Left_CrusII	heathy	244	0.125	0.148	0.0614	0.024	0.0015	-0.455	491	0.649	-0.041
	stroke	249	0.1261	0.148	0.0542	0.026	0.0016				
Vermis_CrusII	heathy	244	0.0043	0.007	0.0011	0.001	0.0001	0.286	491	0.775	0.025
	stroke	249	0.0042	0.01	0.0011	0.002	0.0001				
Right_CrusII	heathy	244	0.0946	0.14	0.0309	0.023	0.0015	-0.224	491	0.822	-0.02
	stroke	249	0.0951	0.158	0.0333	0.024	0.0015				
Left_VIIb	heathy	244	0.0485	0.06	0.0215	0.011	0.0007	-2.673	491	0.008	-0.238
	stroke	249	0.0517	0.086	0.0165	0.015	0.0009				
Vermis_VIIb	heathy	244	0.0019	0.004	0.0004	6E-04	0	-3.878	491	<.001	-0.346
	stroke	249	0.0021	0.004	0.0007	6E-04	0				
Right_VIIb	heathy	244	0.0604	0.064	0.0321	0.012	0.0007	-4.534	491	<.001	-0.404
	stroke	249	0.0658	0.072	0.0297	0.015	0.0009				
Left_VIIIa	heathy	244	0.047	0.062	0.0202	0.011	0.0007	-2.97	491	0.003	-0.265
	stroke	249	0.0506	0.105	0.0134	0.016	0.001				
Vermis_VIIIa	heathy	244	0.0252	0.022	0.014	0.005	0.0003	0.379	491	0.705	0.034
	stroke	249	0.025	0.032	0.0095	0.006	0.0003				
Right_VIIIa	heathy	244	0.0536	0.06	0.0243	0.012	0.0007	-2.031	491	0.043	-0.181
	stroke	249	0.0561	0.075	0.0218	0.016	0.001				
Left_VIIIb	heathy	244	0.0497	0.06	0.0177	0.011	0.0007	2.164	491	0.031	0.193
	stroke	249	0.0473	0.074	0.0172	0.013	0.0008				
Vermis_VIIIb	heathy	244	0.0072	0.011	0.0016	0.002	0.0001	-1.138	491	0.255	-0.102
	stroke	249	0.0074	0.014	0.0011	0.002	0.0002				
Right_VIIIb	heathy	244	0.0489	0.064	0.021	0.012	0.0008	5.94	491	<.001	0.53
	stroke	249	0.0422	0.084	0.0109	0.013	0.0008				
Left_IX	heathy	244	0.0458	0.055	0.018	0.012	0.0008	4.041	491	<.001	0.36
	stroke	249	0.0413	0.073	0.0081	0.013	0.0008				
Vermis_IX	heathy	244	0.0126	0.021	0.0016	0.004	0.0002	-2.328	491	0.02	-0.208
	stroke	249	0.0134	0.024	0.0019	0.004	0.0003				
Right_IX	heathy	244	0.0526	0.07	0.0192	0.014	0.0008	6.483	491	<.001	0.578
	stroke	249	0.0445	0.087	0.0074	0.015	0.0009				
Left_X	heathy	244	0.0075	0.008	0.0044	0.001	0.0001	1.492	491	0.136	0.133
	stroke	249	0.0073	0.01	0.0039	0.002	0.0001				
Vermis_X	heathy	244	0.001	0.003	0	7E-04	0	-5.544	491	<.001	-0.494
	stroke	249	0.0014	0.004	0	9E-04	0.0001				
Right_X	heathy	244	0.0071	0.009	0.004	0.002	0.0001	6.08	491	<.001	0.542
	stroke	249	0.0063	0.008	0.0031	0.002	0.0001				
Left_Total	heathy	244	0.7154	0.571	0.4349	0.099	0.0062	-1.169	491	0.243	-0.104
	stroke	249	0.7264	0.681	0.4624	0.11	0.007				
Right_Total	heathy	244	0.6758	0.654	0.3238	0.107	0.0068	2.3	491	0.022	0.205
	stroke	249	0.6543	0.55	0.4186	0.102	0.0065				
WMV LI	heathy	244	0.03	0.37	-0.064	0.037	0.0024	-6.498	491	<.001	-0.579
	stroke	249	0.0526	0.29	-0.092	0.041	0.0026				

Supplementary Table 3. Partial between Western Aphasia Battery (WAB) language

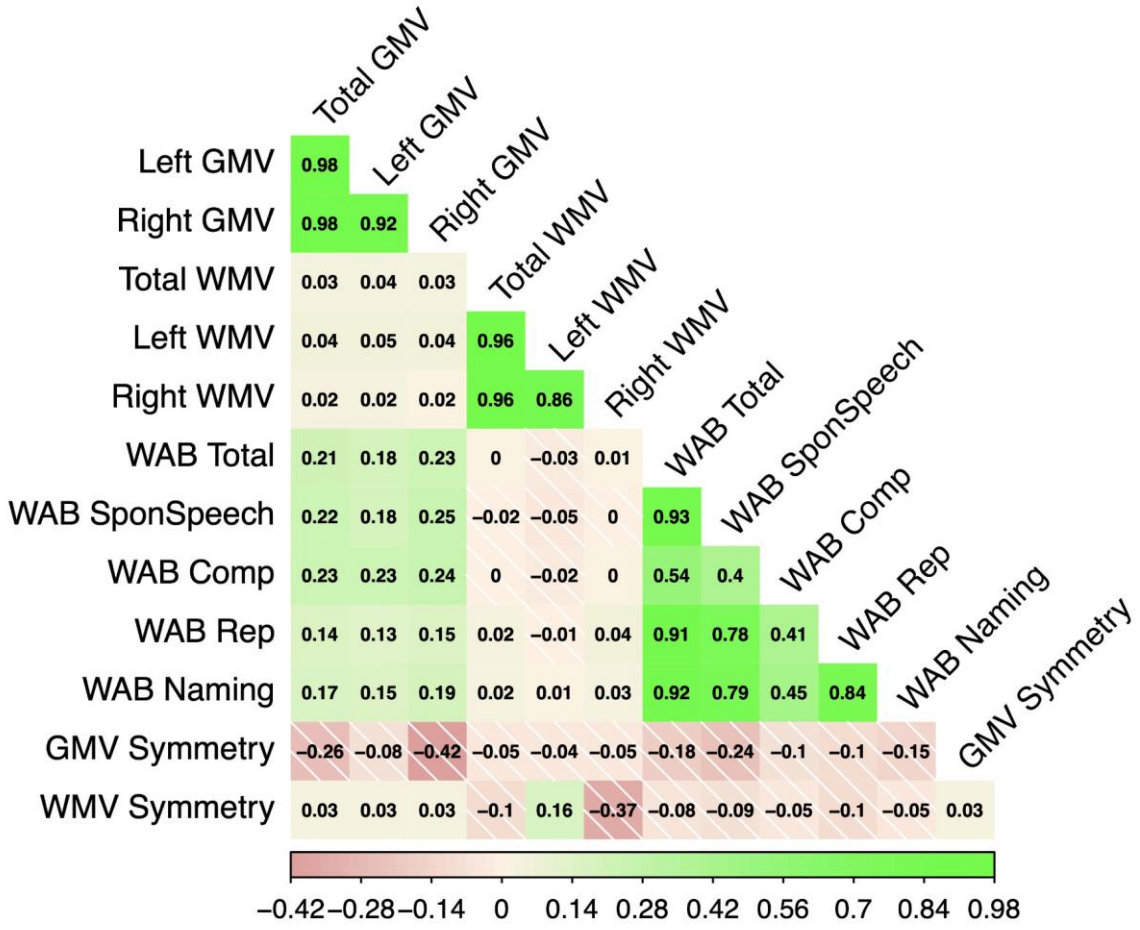

scores and cerebellar measures after controlling for controlling for the effects of age, gender, race, lesion size, and days post-stroke

Supplementary Table 4. Results from a one-way ANOVA comparing linear regression models that used either [demographic variables + cortical lesion data] or [demographic + cortical lesion data + cerebellar GMV] to account for variation in of treatment-related language gains (i.e. changes in the ability to name visually presented objects, i.e.

Treated40 scores). Inclusion of cerebellar GMV significantly improved model fit.

Model Summary – Treated40Gains

Model	R	R^2	Adjusted R^2	RMSE
H_0	0.453	0.205	0.149	4.049
H_1	0.786	0.618	0.309	3.648

Note. Null model includes AGE, daysPostStroke, LesionSizeVoxels, RACE, SEX

ANOVA ▼

Model		Sum of Squares	df	Mean Square	F	p
H_0	Regression	300.667	5	60.133	3.667	0.005
	Residual	1164.216	71	16.397		
	Total	1464.883	76			
H_1	Regression	905.822	34	26.642	2.001	0.017
	Residual	559.061	42	13.311		
	Total	1464.883	76			

Note. Null model includes AGE, daysPostStroke, LesionSizeVoxels, RACE, SEX

Coefficients

Model		Unstandardized	Standard Error	Standardized	t	p	Collinearity Statistics	
							Tolerance	VIF
H_0	(Intercept)	7.846	6.512		1.205	0.232		
	AGE	−0.094	0.040	−0.255	−2.356	0.021	0.956	1.046
	daysPostStroke	-2.469×10^{-4}	2.790×10^{-4}	−0.098	−0.885	0.379	0.906	1.104
	LesionSizeVoxels	-1.569×10^{-5}	5.681×10^{-6}	−0.307	−2.761	0.007	0.906	1.104
	RACE	1.439	1.242	0.124	1.159	0.250	0.984	1.016
	SEX	−2.178	0.949	−0.247	−2.295	0.025	0.966	1.036
H_1	(Intercept)	−24.925	12.186		−2.045	0.047		
	AGE	−0.106	0.057	−0.289	−1.857	0.070	0.376	2.660
	daysPostStroke	-9.666×10^{-6}	3.310×10^{-4}	−0.004	−0.029	0.977	0.522	1.914
	LesionSizeVoxels	-1.339×10^{-5}	8.012×10^{-6}	−0.262	−1.672	0.102	0.370	2.705
	RACE	6.036	1.803	0.518	3.348	0.002	0.379	2.639
	SEX	−1.045	1.248	−0.119	−0.837	0.407	0.453	2.208
	GMV_Left_I_IV	−29.901	66.553	−0.137	−0.449	0.656	0.097	10.270
	GMV_Right_I_IV	−18.078	70.845	−0.090	−0.255	0.800	0.073	13.737
	GMV_Left_V	−61.847	57.747	−0.320	−1.071	0.290	0.102	9.848
	GMV_Right_V	209.755	65.419	1.239	3.206	0.003	0.061	16.444
	GMV_Left_VI	1.729	33.167	0.020	0.052	0.959	0.064	15.736
	GMV_Vermis_VI	−36.564	80.108	−0.085	−0.456	0.650	0.262	3.811
	GMV_Right_VI	−72.853	41.314	−0.856	−1.763	0.085	0.039	25.922
	GMV_Left_CrusI	−29.544	33.214	−0.524	−0.889	0.379	0.026	38.258
	GMV_Vermis_CrusI	−1308.571	1934.201	−0.083	−0.677	0.502	0.598	1.673
	GMV_Right_CrusI	32.687	32.590	0.595	1.003	0.322	0.026	38.745
	GMV_Left_CrusII	−77.227	37.745	−1.011	−2.046	0.047	0.037	26.877
	GMV_Vermis_CrusII	89.843	262.474	0.062	0.342	0.734	0.273	3.663
	GMV_Right_CrusII	52.768	37.681	0.767	1.400	0.169	0.030	32.980
	GMV_Left_VIIb	−5.197	49.765	−0.044	−0.104	0.917	0.052	19.218
	GMV_Vermis_VIIb	999.164	603.632	0.301	1.655	0.105	0.274	3.644
	GMV_Right_VIIb	8.935	57.644	0.076	0.155	0.878	0.038	26.159
	GMV_Left_VIIIa	−38.151	61.619	−0.290	−0.619	0.539	0.042	24.066
	GMV_Vermis_VIIIa	319.179	185.837	0.461	1.718	0.093	0.126	7.920
	GMV_Right_VIIIa	19.932	70.608	0.154	0.282	0.779	0.030	32.892
	GMV_Left_VIIIb	−67.960	59.123	−0.408	−1.149	0.257	0.072	13.862
	GMV_Vermis_VIIIb	−488.766	310.392	−0.442	−1.575	0.123	0.115	8.685
	GMV_Right_VIIIb	62.646	60.515	0.373	1.035	0.306	0.070	14.302
	GMV_Left_IX	−13.874	71.906	−0.077	−0.193	0.848	0.057	17.688
	GMV_Vermis_IX	177.213	219.459	0.267	0.807	0.424	0.083	12.013
	GMV_Right_IX	104.288	76.436	0.617	1.364	0.180	0.044	22.539
	GMV_Left_X	170.568	210.857	0.170	0.809	0.423	0.205	4.882
	GMV_Vermis_X	−457.636	363.310	−0.262	−1.260	0.215	0.210	4.766
	GMV_Right_X	157.635	227.134	0.155	0.694	0.491	0.181	5.516
	GAsymmetryInd	154.205	133.012	0.981	1.159	0.253	0.013	78.811

Supplementary Methods:

Imaging

T1-weighted structural images collected from individuals with chronic stroke were enantiomorphically healed prior to Cat12 preprocessing. This technique, originally described by Nachev and colleagues(Nachev et al., 2008), involves replacing damaged areas in the lesioned hemisphere (LH in this case) with data from the healthy hemisphere (RH in this case). After healing, the image can be input into standard normalization procedures which warp the individual's brain to any standard 3D brain template (i.e. MNI, SPM, FSL). Without the healing process, the normalization procedure typically fails catastrophically (especially for larger regions which deviate from probabilistic maps of WM and GM), and in unpredictable ways(Nachev et al., 2008). This approach has been used in multiple studies in stroke, including studies from our lab(Basilakos et al., 2019; Rorden et al., 2009; Suarez et al., 2020; Wilmskoetter et al., 2021; Yourganov et al., 2015, 2018), and is embedded in our stroke-specific image processing pipeline, *nii_preprocess(Rorden et al., 2020)*.

Additional Analyses

We conducted a series of exploratory Pearson's correlations to examine the relationship between demographic data and our primary dependent variables of interest, cerebellar

volume and asymmetry as illustrated in Supplementary Tables 1A and 1B. In all analyses subsequently reported we controlled for age, gender and race.

Language Measures

Western Aphasia Battery (WAB)

For all C-STAR treatment studies, aphasia severity was computed by trained speech-language pathologists based on administration of the Western Aphasia Battery (WAB) or Western Aphasia Battery-Revised (WAB-R)(Kertesz, 2022). Total WAB scores, as well as subscores for spontaneous speech, object naming, speech repetition, and speech comprehension were calculated according to the manual. WAB scores were typically measured at intake (participant recruitment) in order to ensure they were eligible to participate in available studies which only accepted participants with WAB total scores indicating presence of aphasia.

Object Naming Task (Treated40)

The *Treated40* variable represents treatment related gains experienced by participants in various C-STAR intervention studies (N = 77). Participants included in this group completed sparse fMRI scanning sessions at multiple timepoints at the McCausland

Center for Brain Imaging (MCBI) located at Palmetto Richland Heart Hospital, Columbia, SC. During these 10-minute thirty-second sparse fMRI scans, individuals with chronic stroke were presented with 40 pictures of concrete objects and 40 pictures of abstract art. Pictures were viewed through a mirror placed directly above the participants eyes. Participants were instructed to name objects they recognized and remain silent when abstract pictures were presented. Speaking occurred during the off period of the scans (silent periods) and fMRI images were collected during quiet periods. Audio recordings made during the silent portion of the sparse fMRI scans, acquired using a Serene Sound MRI Compatible Audio System, were manually scored by trained speech-language pathologists offline. *Treated40* accuracy gains were calculated as:

[# pictures correctly identified after treatment] - [# of pictures correctly identified before treatment]

with higher numbers indicating greater pre-post improvement. Additional details regarding the *Treated40* task, its administration, and properties can be found here(Fridriksson et al., 2009).

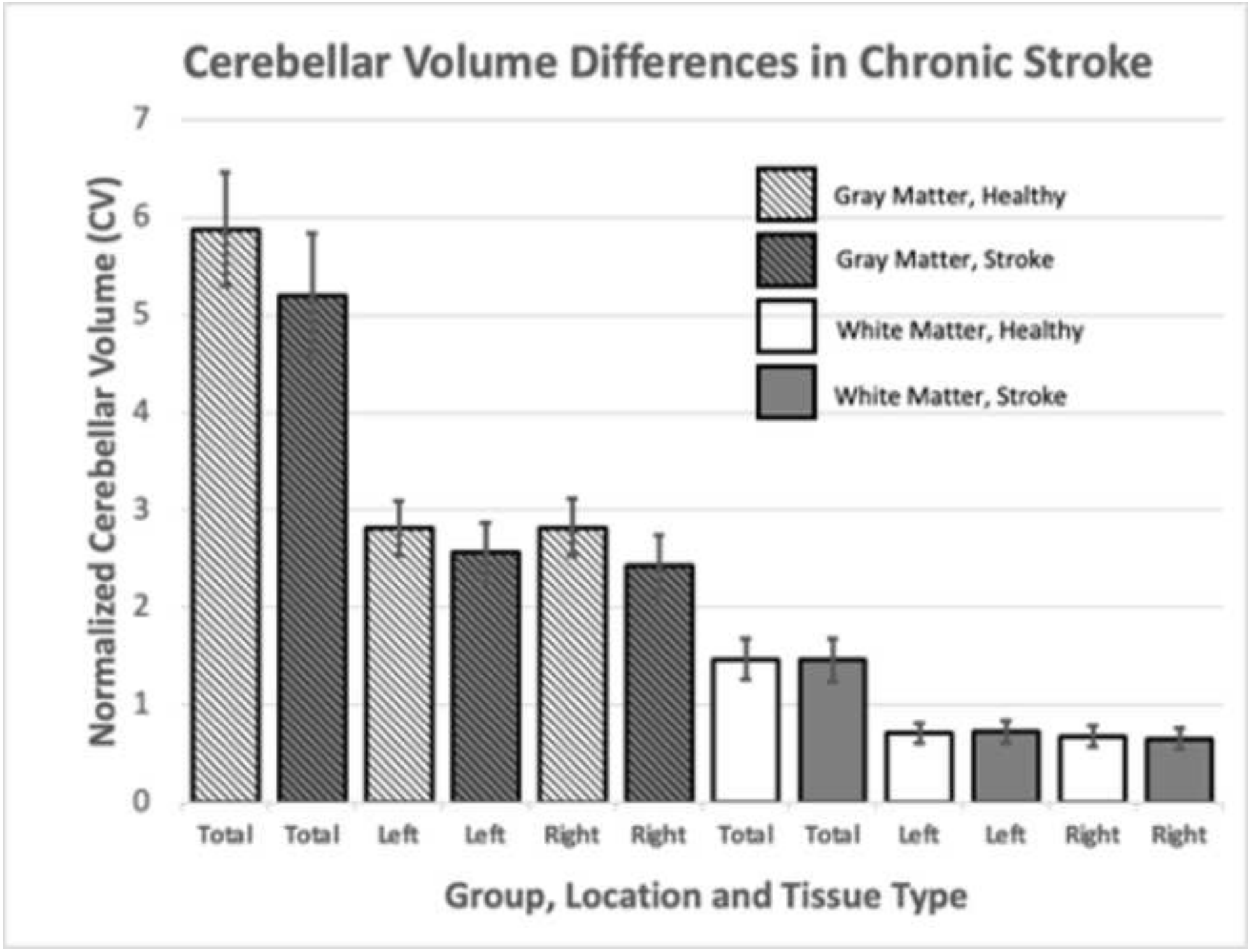

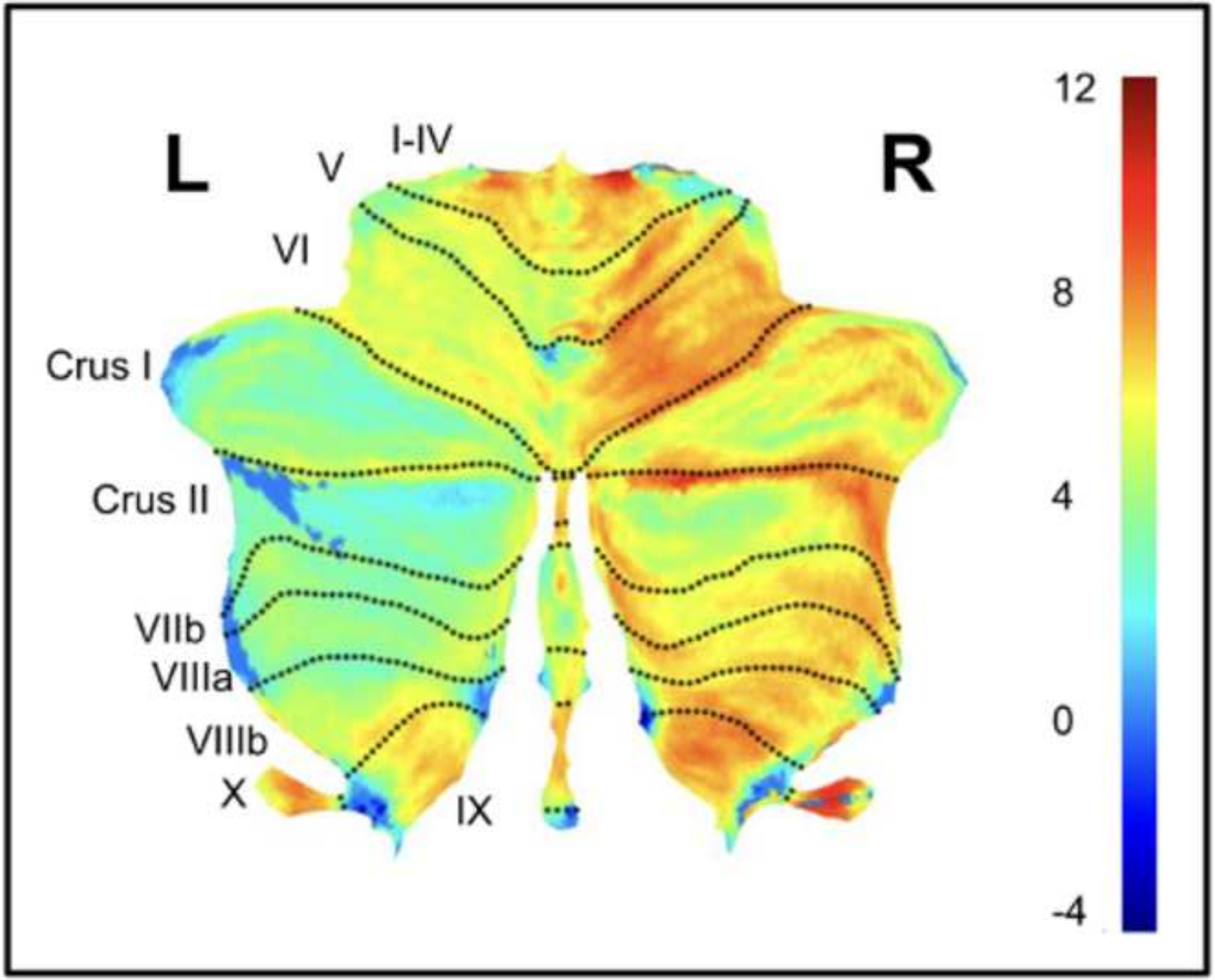

Figure3

Click here to access/download;Figure;Figure3.png